

## Virus- and bactericidal LED lamp with increased efficiency

**Abstract.** Recently available on the market, LED UV-C diodes enable the construction of bactericidal and virucidal diode "bulbs" (lamps with E14 and E27 bases). Usually these are only slightly modified ordinary white light LED lamps. The following text describes simple and inexpensive modifications to the power supply system, which will increase the efficiency and life of the UV-C LED lamp and may increase its operational effectiveness.

**Streszczenie.** Obecnie od niedawna na rynku diody LED UV-C umożliwiają konstruowanie bakterio- i wirusobójczych „żarówek” diodowych (lamp z trzonkiem E14 i E27). Zazwyczaj są to tylko w niewielkim stopniu przerobione zwykłe lampy LED światła białego. W tekście poniżej opisano proste i niedrogie modyfikacje układu zasilającego, które przyczynią się do zwiększenia sprawności i żywotności lampy LED UV-C oraz mogą podwyższyć skuteczność jej działania. (Wiruso- i bakterioobójcza lampa LED o podwyższonej skuteczności działania).

**Keywords:** SSL, LED lamp, UV-C LED, Index Flicker, pulsed UV-C.

**Słowa kluczowe:** lampa LED, dioda UV-C, wskaźnik migotania, pulsacyjne UV-C.

### Introduction

Solid-state lighting (SSL) sources based on light-emitting diodes (LED) are very widely used today. Among many varieties of LEDs, manufacturers offer also virus- and bactericidal UV-C LED lamps as replacements for low-pressure mercury discharge lamps with E14 and E27 bases. The interest in UV-C LEDs has been greatly increased during the recent pandemic as a measure against the coronavirus SARS-CoV-2 [1]. Efficient semiconductor sources of UV-C radiation have been developed recently [2] in order to eliminate environmentally hazardous mercury lamps. Usually, these UV-C LEDs are only slightly modified ordinary LED lamps, in which white light-emitting diodes have been replaced with diodes emitting UV-C radiation. The modifications applied by the manufacturers are most often limited to decreasing the number of series connected diodes in order to adjust the total voltage drops to the existing power supply system (UV diodes are characterized by a significantly higher forward voltage). Such structures are very versatile, easy to use and (in case of damage) easily replaceable compared to the systems in which the LED modules form one unit with the luminaire. The construction of an LED lamp in a luminaire resembling an ordinary light bulb requires solving a number of significant problems [3]. First of all, the small space and high temperature inside the bulb with an E14 or E27 base make it difficult to use solutions based on switching converters. The interior of such a lamp, with a power of several watts or more, often heats up to a temperature exceeding 100°C. While the durability of modern LEDs at such a high temperature is still acceptable, the problem is with other electronic components. Electrolytic capacitors and magnetic elements (chokes in filters and transformers) cannot either work at such high temperatures (e.g. exceeding the Curie point), or their essential parameters deteriorate significantly. At high temperatures, due to drying up the durability of electrolytic capacitors shortens dramatically and the losses in magnetic elements significantly increase.

Figure 1a shows a schematic diagram of a typical LED lamp. It consists of a rectifier, a single string of LEDs connected in series, and an IC regulator that stabilizes the current flowing through the diodes. The operation of the system is very simple. At the moment  $t_{ON}$ , when the rectified 230VAC mains voltage exceeds the value of the LED chain voltage ( $n \cdot U_F$ ), the current regulator becomes biased and a constant current  $I_A$  starts flowing. A further increase of the input voltage does not change the current and the excess voltage, i.e.  $U_{CS} = U_R - n \cdot U_F$ , appears across the regulator.

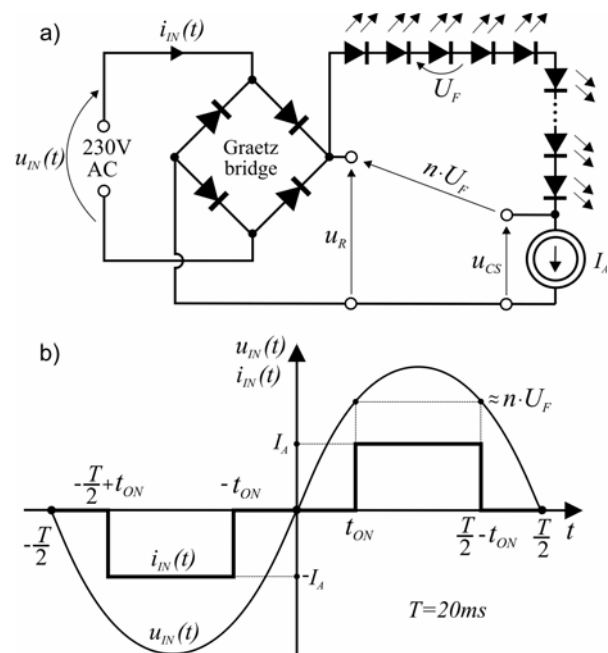


Fig. 1. Circuit diagram of a single chain LED lamp (a) and the waveforms of current and voltage at its input (b)

Adequate waveforms are presented in figure 1b. From the point of view of the LED lamp designer, the most important thing is to choose the appropriate length of the LED chain, which has a direct effect on the value of time  $t_{ON}$ . The works [4, 5] show the dependence of important electrical parameters of the lamp on the value of time  $t_{ON}$  and the current  $I_A$ . In the whole range of possible settings  $t_{ON}$  (0 - 5ms), due to the requirements of the standards related to the EMC directive [6], it cannot exceed 2.53ms. In turn, a value too low will radically reduce the energy efficiency of the lamp. A good compromise is to take the value of  $t_{ON} \approx 2.26ms$  [5]. When examining LED lamps available on the market, it can be noticed that many manufacturers, however, adopt much lower  $t_{ON}$  values (1.7 - 1.9ms, typically) in their designs. This applies to both lamps that emit white light, as well as infrared and ultraviolet. Apart from the possible ignorance of designers (at  $t_{ON} \approx 2.26ms$  the energy efficiency is higher by about 1/5 compared to  $t_{ON} \approx 1.7ms$ , therefore the lamp can obtain a higher energy efficiency class), shortening  $t_{ON}$  significantly

below the optimal value can be explained by the wish to ensure better stability of the light flux of the LED lamp. Lamps with periodically unstable white light flux may cause a troublesome flickering effect (if the pulsing frequency is low) or cause stroboscopic effects. The scale of these effects can be estimated using two parameters that have been developed quite a long time ago, but are still in common use, i.e. Flicker Percent and Flicker Index [7]. Figure 2 shows the curves of the values of these parameters and the energy efficiency of the LED supply system [5] depending on the time  $t_{ON}$ .

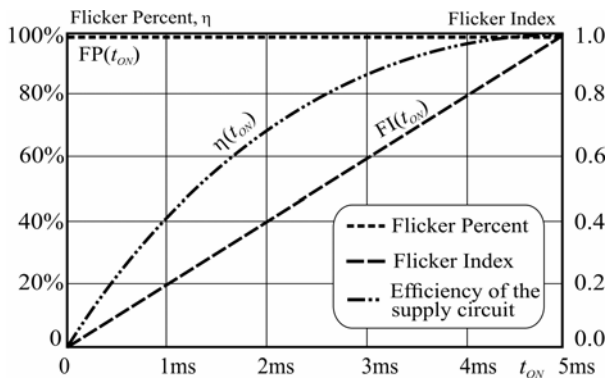


Fig. 2. Graphs of parameters Flicker Percent, Flicker Index and energy efficiency of the power supply system for the LED lamp in figure 1a as functions of  $t_{ON}$

The parameter Flicker Percent turns out to be completely useless for the assessment of the cyclic instability of the luminous flux of lamps in which the instantaneous value of the flux drops to zero. In each such lamp, regardless of the length of time in which the light flux remains extinguished, Flicker Percent will assume the highest, i.e. the worst, value of 100% [8]. The situation is different with the Flicker Index. Here, the area (time integral for one period) of the light flux above the averaged value of this flux to its total area is assessed. For a perfectly stable light, the Flicker Index value will be zero, while for a source emitting light in the form of short flashes, the Flicker Index will be close to one. The pursuit of a low Flicker Index is perfectly understandable. In the case of white light, it will be more comfortable for the eyes.

However, the above considerations cannot apply to UV-C lamps. UV-C radiation is very harmful to the eyes and cannot be used in the presence of humans and animals. There is no rational justification for using non-optimal power systems (i.e. with  $t_{ON}$  smaller than 2.26ms) to obtain a low Flicker Index value in LED UV-C lamps. The existence of such lamps, where  $t_{ON} \approx 1.7 \dots 1.9$ ms, can only be explained by the desire to easily use the white light LED power supply system previously developed by the manufacturer, which has already obtained the required certificates for compliance with the EMC directive.

Contrary to lighting applications, the use of intense and short UV pulses to inactivate microorganisms has an advantage over continuous illumination by providing a significantly higher level of inactivation without requiring long exposure times. However, even with large instantaneous power of such pulses, the problem of the so called photoreactivation after exposing the microorganisms back to visible light still exists [9], so systems with continuous emissions are still popular [1, 10].

The disinfecting efficiency of UV-C lamps depends on the time and the average power of the radiation emitted by them per unit area. It turns out, however, that not only the averaged power value, but also the waveform itself may

have a significant effect on the ability to destroy pathogens. The work [11] presents the comparative results of the effectiveness of the discharge UV-C lamp and the LED UV-C lamp. The authors of the study explained the higher efficiency of the LED UV-C lamp, among others, by using a different method of regulating and modulating the radiation of LED UV-C diodes, i.e. by using PWM regulation. By supplying LEDs with a rectangular current waveform (PWM modulation), it is possible to emit radiation with many times greater instantaneous power, while maintaining the same average power value. It is also worth emphasizing that in discharge lamps the possibility of shaping the waveform of the emitted radiation is greatly reduced comparing to systems with LEDs. This limitation results mainly from the need to use high voltage to initiate the operation of the discharge lamp, as well as the requirement to heat and maintain the proper temperature of the filaments.

To sum up, a probable thesis can be made that in the case of two sources of UV-C radiation, with the same spectral characteristics and average power, more effective in destroying pathogens (e.g. creating pyrimidine dimers that degrade RNA and DNA chains) will be the source emitting radiation from periodically higher value of instantaneous power [12]. When designing a power supply system for such a source, it is necessary to ensure emission in which the ratio of the maximum instantaneous power to the average power will be large. Relating the above considerations to LED power supply systems, it would be advisable to develop a solution ensuring the value of the Flicker Index parameter as high as possible (i.e. contrary to the recommendations for LED supply systems in white light lamps).

#### Possible modifications of the power supply system for the UV-C LEDs

Each electrical system connected to the 230VAC network must meet the requirements of specific standards. In the case of lamps with a rectangular supply current waveform, the most difficult conditions to meet are the conditions specified in the PN-EN IEC 61000-3-2 standard [6]. These regulations specify the maximum allowable levels of input current harmonics, depending on the power and type of load connected to a single-phase 230VAC network. According to the mentioned standard, lamps are classified as very restrictive class C. However, chapter 7.4.3 presents the relaxed criteria for lamps with an active power in the range of 5 - 25W. According to these provisions, it is necessary to meet at least one of the three groups of requirements. For the rectangular shape of the input current waveform, the set presented in the third group of requirements is the most appropriate. According to it, the total THD content of the supply current should not be greater than 70%, while the amplitudes of the specified harmonics in proportion to the amplitude of the fundamental harmonic should not exceed: the second harmonic 5%, the third 35%, the fifth 25%, the seventh 30%, and the ninth and eleventh 20%.

It was shown in [5] that the rectangular waveform of the supply current (fig. 1b) does not have even harmonics, while the odd harmonics are defined by the formula:

$$(1) \quad B_k = 4 \cdot \frac{I_A}{k\pi} \cdot \cos k\omega t_{ON}$$

for  $k = 1, 3, 5, 7, 9, 11, \dots$ , where:  $|B_k|$  - odd harmonic amplitudes,  $\omega$  - pulsation of 230VAC mains. The proportion of successive harmonics in relation to the fundamental harmonic amplitude ( $B_k/B_1$ ) is defined by expression (2). The negative value of this expression, which will occur for

certain ranges of  $t_{ON}$ , signals a phase shift of 180 degrees of the  $k$ -th harmonic with respect to the fundamental.

$$(2) \quad B_k/B_1 [\%] = \frac{\cos k\omega t_{ON}}{k \cdot \cos \omega t_{ON}} \cdot 100\%$$

for  $k = 3, 5, 7, 9, 11$ . On the other hand, the  $THD$  value is described by formula (3):

$$(3) \quad THD = \frac{\sqrt{I_{RMS}^2 - \frac{B_1^2}{2}}}{\frac{B_1}{\sqrt{2}}} = \sqrt{\frac{\frac{\pi^2}{8} \left(1 - 4 \frac{t_{ON}}{T}\right)}{\cos^2 \omega t_{ON}} - 1}$$

where:  $I_{RMS}$  - RMS input current,  $B_1$  - first harmonic amplitude,  $T = 20\text{ms}$  - 230VAC mains voltage period.

Figure 3 shows the graphs of  $THD$  changes and the percentage  $B_k/B_1$  ratios depending on the value of  $t_{ON}$ .

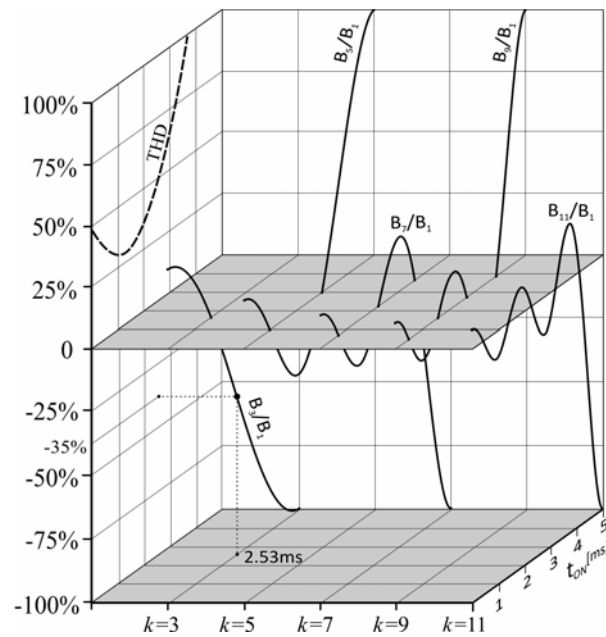


Fig. 3. Graphs of  $THD$  and  $B_k/B_1$  as functions of  $t_{ON}$

Analyzing plots from figure 3 it is easy to notice that for the LED supply system from figure 1a the maximum value of  $t_{ON}$  is 2.53ms. At this value one of the conditions mentioned in the standard is exceeded, i.e.  $|B_3/B_1| > 0.35$ . Modification of the power supply system, which will allow to increase  $t_{ON}$  above 2.53ms, would be very desired. The greater energy efficiency and larger value of the Flicker Index will improve the operation of the UV-C LED lamp. One of the possible solutions is presented in figure 4.

The waveform of the input current is composed of two rectangular components, namely  $i_{IN}(t) = i'_{IN}(t) + i''_{IN}(t)$ . It is obvious that the harmonics of the final waveform are a sum of the harmonic waveforms of the components. Assuming equal weights ( $1/2$ ) with which the components affect the final values, i.e.  $B_k/B_1 = 1/2 \cdot B'_k/B'_1 + 1/2 \cdot B''_k/B''_1$ , it is necessary to satisfy the condition  $1/2 \cdot B_1 = B'_1 = B''_1$ , which may be presented with equation (4):

$$(4) \quad \frac{I_B}{I_A} = \frac{\cos \omega t_1}{\cos \omega t_2}$$

where:  $t_1$  - the beginning of the step with a height  $I_A$  in the waveform  $i_{IN}(t)$ ,  $t_2$  - the beginning of the step  $I_A + I_B$ .

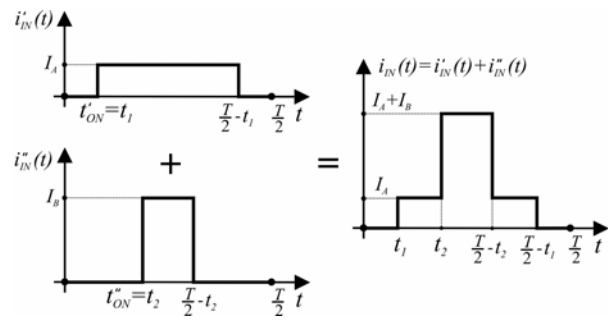


Fig. 4. Modification of the waveform  $i_{IN}(t)$  to obtain  $t_2 > 2.53\text{ms}$

In the analysis of the harmonics of the two-step waveform we can consider the sum of the harmonics of two single-step waveforms, and after taking into account the sign of each of them (i.e. phase shift 0 or 180 degrees), determine the ranges of allowed changes of  $t_1$  and  $t_2$  for which the relevant conditions on  $B_k/B_1$ , as specified in the standard [6], are satisfied. However, the same method should not be used when determining the  $THD$ . The value of nonlinear distortions of the waveform  $i_{IN}(t)$  from figure 4 will differ from the summed  $THD$  values of the component waveforms  $i'_{IN}(t)$  and  $i''_{IN}(t)$ . Formula (5) determines the  $THD$  for the two-step waveform under the conditions for  $I_A$  and  $I_B$  defined by formula (4).

$$(5) \quad THD = \sqrt{\frac{\pi^2}{32} \left( \frac{1 - 4 \frac{t_1}{T}}{\cos^2 \omega t_1} + \frac{1 - 4 \frac{t_2}{T}}{\cos^2 \omega t_2} + 2 \cdot \frac{1 - 4 \frac{t_2}{T}}{\cos \omega t_1 \cdot \cos \omega t_2} \right) - 1}$$

The ranges of  $t_1$  and  $t_2$ , for which the third set of requirements from chapter 7.4.3 of the standard [6] is met, were determined using numerical methods. The value of  $t_1$  was changed from 0 to 5ms every  $10\mu\text{s}$ , while  $t_2$  from  $t_1$  to 5ms, also every  $10\mu\text{s}$ . For each pair  $t_2$  and  $t_1$ , successive values of  $B_k/B_1$  and  $THD$  were calculated. Fig. 5 shows the area of allowed changes  $t_2$  and  $t_1$  with a dark gray shade for which the requirements of the standard are met.

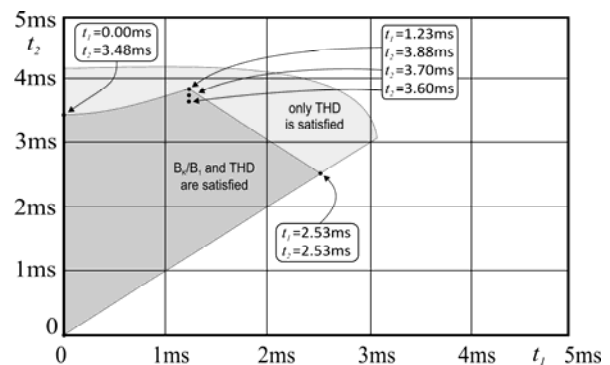


Fig. 5. Range of change of  $t_1$  and  $t_2$ , for which the third set of requirements in chapter 7.4.3 of the standard [6] is satisfied

To obtain the highest value of  $t_2$ , the pair  $t_1 = 1.23\text{ms}$  and  $t_2 = 3.88\text{ms}$  should be selected. Unfortunately, in this choice there is a very small margin to the limits specified in the standard [6]. The additional points marked on the graph (fig. 5) ( $t_1 = 1.23\text{ms}$  and  $t_2 = 3.70\text{ms}$  as well as  $t_1 = 1.23\text{ms}$  and  $t_2 = 3.60\text{ms}$ ) allow this margin to be increased. In real systems, however, the situation is more favourable than in theoretical considerations. The waveforms of the current  $i_{IN}(t)$  are less steep compared to the idealized mathematical

description. This translates into lower amplitudes of higher harmonics, and thus lower values of  $|B_k/B_1|$  [5].

Another important parameter to determine is the energy efficiency of the power supply system, defined as the percentage ratio of the power transferred to the LEDs to the total active power drawn from the 230VAC network. The principle of white light LED operation is based on partial conversion of blue light ( $\lambda \approx 450\text{nm}$ ) through the yellow phosphor. Losses resulting from such conversion reduce the efficiency of the LED (i.e. the ratio of the emitted power within the desired radiation range to the electric power consumed). Energy transformations taking place in the diodes emitting monochromatic radiation (infrared, coloured light and ultraviolet) can be much more effective. During operation such a lamp heats up to a temperature which will depend to a much greater extent on the efficiency of the power supply system than in the case of white light lamps. Power systems with higher energy efficiency will lower the temperature and thus extend the life of the UV-C LEDs.

Formula (6) determines the energy efficiency  $\eta$  of the power supply system with a two-step waveform  $i_{IN}(t)$ . When deriving it, the following assumptions were made: the values  $I_A$  and  $I_B$  meet the conditions defined by formula (4), while the current regulators operate correctly from the minimum voltage value  $U_{CS}$  (i.e.  $U_{CSmin} \approx 0$ ).

(6)

$$\eta = \pi \cdot \left( \frac{t_2 - t_1}{T} \tan \omega t_1 + \left( \frac{1}{4} - \frac{t_2}{T} \right) \cdot \left( \frac{\sin \omega t_2}{\cos \omega t_1} + \tan \omega t_2 \right) \right) \cdot 100\%$$

The calculated values of important parameters for LED lamps with active power up to 25W are presented in table 1. Significantly higher values of  $P_{MAX}/P_{AVR}$  (periodic maximum instantaneous power supplied to the LEDs in relation to the average power) and energy efficiency  $\eta$  were obtained than would be possible in the classic system shown in figure 1a.

Table 1. Values of significant parameters for selected pairs of  $t_1$  and  $t_2$

| $t_1 = t_2 =$<br>[ms] | $\frac{B_3}{B_1}$ | $\frac{B_5}{B_1}$ | $\frac{B_7}{B_1}$ | $\frac{B_9}{B_1}$ | $\frac{B_{11}}{B_1}$ | $\frac{I_A + I_B}{I_A}$ | $\frac{P_{MAX}}{P_{AVR}}$ | $\eta$<br>[%] |
|-----------------------|-------------------|-------------------|-------------------|-------------------|----------------------|-------------------------|---------------------------|---------------|
| 1.23<br>3.88          | -0.349            | 0.247             | -0.20             | -0.06             | 0.07                 | 3.69                    | 3.55                      | 82.7          |
| 1.23<br>3.70          | -0.32             | 0.19              | -0.12             | -0.13             | 0.09                 | 3.33                    | 3.12                      | 83.2          |
| 1.23<br>3.60          | -0.31             | 0.15              | -0.08             | -0.15             | 0.08                 | 3.18                    | 2.92                      | 83.4          |

## Summary

Scientific research carried out for the processing industry and food technology confirms the high efficiency of UV lamps, in which the emission of radiation is in the form of short pulses of high instantaneous power [9, 12, 13]. The use of UV-C LEDs in disinfection lamps with a properly designed control and power supply system will contribute to more effective inactivation of pathogens.

The modifications to the UV-C LED power supply system proposed in this paper will allow for shorter radiation pulses with a higher instantaneous power and will contribute to increasing the effectiveness and improvement of the energy efficiency of the disinfection lamp. The diagram of the simplest solution, using the same elements as in the classic system, is shown in figure 6.

By choosing the chain lengths of UV-C LEDs (setting  $t_1$  and  $t_2$ ), as well as the values of the currents  $I_A$  and  $I_B$ , we will get a system with the desired two-step supply current waveform.

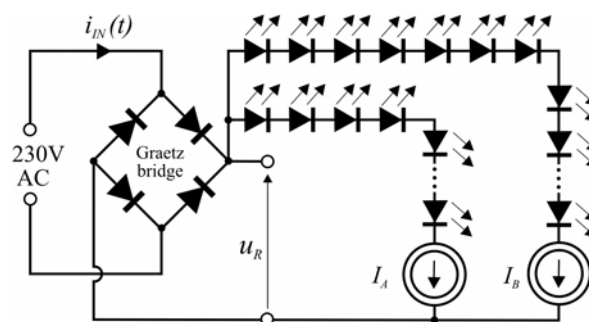


Fig. 6. Example circuit diagram of a simple UV-C LED lamp with a two-step waveform of the current  $i_{IN}(t)$

However, it should be noted that due to the simultaneous conduction of both diode branches within the interval  $t_2 < t < \frac{1}{2}T - t_2$ , the efficiency of such a simple system will be lower than the achievable values given in table 1.

**Authors:** Jacek Chęciński, PhD, Zdzisław Filus, PhD, DSc, prof. SUT, Silesian University of Technology, Department of Electronics, Electrical Engineering and Microelectronics, ul. Akademicka 16, 44-100 Gliwice, E-mails: [jacek.checinski@polsl.pl](mailto:jacek.checinski@polsl.pl), [zdzislaw.filus@polsl.pl](mailto:zdzislaw.filus@polsl.pl)

## REFERENCES

- Juarez-Leon F.A., Soriano-Sanchez A.G., Rodriguez-Licea M.A., Perez-Pinal F.J., Design and Implementation of a Germicidal UVC-LED Lamp, *IEEE Access*, 8 (2020), 196951-196962
- Muramoto Y., Kimura M., Nouda S., Development and future of ultraviolet light-emission, *IEEE Summer Topicals Meeting Series (SUM)*, (2015)
- Li S., Tan S-C., Lee C-K. et al, A survey, classification, and critical review of light-emitting diode drivers, *IEEE Transactions on Power Electronics*, 31 (2016), n.2, 1503-1515
- Filus Z., Chęcinski J., Some remarks on design of LED lamps and their AC direct drivers, *Elektronika ir Elektrotechnika*, 25 (2019), n.3, 39-42
- Chęcinski J., Filus Z., Analysis of supply parameters of single- and double-string LED lamps with integrated AC direct capacitorless drivers, *Bulletin of the Polish Academy of Sciences: Technical Sciences*, 68 (2020), n.4, 819-827
- Standard PN-EN IEC 61000-3-2:2019-04/A1:2021-08 Electromagnetic Compatibility (EMC) – Part 3-2: Limits for harmonic current emissions (equipment input current  $\leq 16$  A per phase)
- Castro I., Vazquez A., Arias M. et al, A review on flicker-free ac-dc LED drivers for single-phase and three-phase ac power grids, *IEEE Transactions on Power Electronics*, 34 (2019), n.10, 10035-10057
- Chęcinski J., Filus Z., Stabilność strumienia światła lamp LED zasilanych z sieci 230 VAC, *Przegląd Elektrotechniczny*, 94 (2018), nr 8, 5-8
- Lamont Y., MacGregor S.J., Anderson J.G., Fouracre R.A., Effect of visible light exposure on E.coli treated with pulsed UV-rich light, *26th International Power Modular Symposium and High Voltage Workshop*, San Francisco, (2004), 619-622
- Santhosh R., Yadav S., Low Cost Multipurpose UV-C Sterilizer box for protection against COVID'19, *International Conference on Artificial Intelligence and Smart Systems (ICAIS-2021)*, Coimbatore, India, (2021), 1495-1498
- Grzesiak W., Guzdek P., Kulawik J. et al, Półprzewodnikowe źródła promieniowania UV-C LED dla potrzeb wybranych procedur stosowanych w technologii żywności, *Przegląd Elektrotechniczny*, 97 (2021), nr 2, 28-31
- Ozer, N. P., Demirci, A., Inactivation of Escherichia coli O157:H7 and Listeria monocytogenes inoculated on raw salmon fillets by pulsed UV- light treatment, *International journal of food science and technology*, 41(4), (2006), 354-360
- Söbeli, C., Uyarcan, M., Kayaardi, S., Pulsed UV-C radiation of beef loin steaks: Effects on microbial inactivation, quality attributes and volatile compounds, *Innovative Food Science and Emerging Technologies*, 67 (2021)